

This discussion paper is/has been under review for the journal Earth Surface Dynamics (ESurfD).
Please refer to the corresponding final paper in ESurf if available.

Tectonic and climatic controls on the Chuquibamba landslide (western Andes, southern Peru)

A. Margirier¹, L. Audin^{1,2}, J. Carcaillet¹, and S. Schwartz¹

¹ISTerre, Université Grenoble I, CNRS, 1381 rue de la piscine, 38400 Grenoble CEDEX 09, France

²IRD, ISTerre, 1381 rue de la piscine, 38400 Grenoble CEDEX 09, France

Received: 23 October 2014 – Accepted: 26 November 2014 – Published: 12 December 2014

Correspondence to: A. Margirier (audrey.margirier@ujf-grenoble.fr)

Published by Copernicus Publications on behalf of the European Geosciences Union.

Title Page

Abstract

Introduction

Conclusions

References

Tables

Figures



Back

Close

Full Screen / Esc

Printer-friendly Version

Interactive Discussion



Abstract

The contribution of landslides to the Quaternary evolution of reliefs is poorly documented in arid contexts. In southern Peru and northern Chile several massive landslides disrupt the arid western Andean front. The Chuquibamba landslide, located in southern Peru, belongs to this set of large landslides. In this area, the Incapuquio fault system captures the intermittent drainage network and localizes rotational landslides. Seismic activity is significant in this region with recurrent $M_w = 9$ subduction earthquakes, however none of the latest seismic events have triggered a major landslide. New terrestrial cosmogenic dating of the Chuquibamba landslide provides evidence that the last major gravitational mobilization of these rotational landslide deposits occurred at ~ 102 ka, during the Ouki wet climatic event identified on the Altiplano between 120 and 98 ka. Our results suggest that wet events in the arid and fractured context of the Andean forearc induced these giant debris-flows. Finally, our study highlights the role of tectonics and climate on (i) the localization of large Andean landslides and on (ii) the long-term mass transfer to the trench along the arid Andean front.

1 Introduction

In active mountain ranges, landslides are an important process in long-term erosion and thus contribute to the geomorphologic evolution of reliefs (Korup et al., 2007). Despite their importance in terms of hazards, landslide maps remain rare (Guzzetti et al., 2012) and information on the type, age or distribution of individual landslide is often lacking. Only a few publications deal with landslide triggering and/or evolution in arid contexts such as the western Andean flank, where several gigantic scarps disrupt the forearc piedmont (Audin and Bechir, 2006; Pinto et al., 2008; Strasser and Schlunegger, 2005; Wörner et al., 2002; Mather et al., 2014; Crosta et al., 2015). In contrast, because of the potential seismotectonic trigger (Keefer, 1984 and 2002), landslide triggering along subduction active margins has been studied for a number of years, but most

ESURFD

2, 1129–1153, 2014

Tectonic and climatic

A. Margirier et al.

Title Page

Abstract

Introduction

Conclusions

References

Tables

Figures

◀

▶

◀

▶

Back

Close

Full Screen / Esc

Printer-friendly Version

Interactive Discussion



Tectonic and climatic

A. Margirier et al.

Title Page

Abstract

Introduction

Conclusions

References

Tables

Figures

◀

▶

◀

▶

Back

Close

Full Screen / Esc

Printer-friendly Version

Interactive Discussion



previous studies focused on humid climatic settings (Taiwan, New Zealand, Papua New Guinea, Japan; Meunier et al., 2008; Hovius et al., 2011). In southern Peru, the topographic gradient (average slope of 4 % between the coast and the Western Cordillera), the crustal seismotectonic activity and the aridity of the forearc region has been directly linked to the Andean uplift and the subduction of the Nazca plate for the last 25 Myrs at least (Devlin et al., 2012; Alpers and Brimhall, 1988; Dunai et al., 2005). However, the Quaternary tectonic crustal activity and its role in the localization of landslides along the western Andean Escarpment has never been explored in southern Peru and northern Chile. As a consequence, numerous questions remain concerning the importance of giant landslides in slope erosion, relative to other nonseismic agents of erosion such as climatic forcing. The “Chuquibamba landslide” is a large complex zone of imbricated landslides (about 80 km²) affecting the Western Cordillera in southern Peru. It belongs to the Andean arid piedmont where most of the geomorphic markers are well preserved from erosion/transport processes (Hall et al., 2008). This study of the Chuquibamba landslide aims to explore the links between seismotectonic activity and abrupt climatic changes on the triggering and development of large landslides. In this paper we map out the area and characterize the tectonic and geomorphological settings, use Terrestrial Cosmogenic Nuclides (TCN) to date pertinent markers of the last debris-flow event and document the evolution of such a landslide area.

2 Context**2.1 Geologic and climatic setting of Chuquibamba region**

The Andean Pacific arid front comprises different morphological units: the Coastal Cordillera 0–1000 m above sea level (a.s.l.), the Pacific Piedmont 1000–1500 m a.s.l. and the Western Cordillera 1500–6000 m a.s.l. In southern Peru, the Western Cordillera corresponds to a Jurassic to Cretaceous volcanic arc (Atherton et al., 1985) (Fig. 1). These magmatic and volcano-sedimentary rocks are emplaced on a Precambrian to

Tectonic and climatic

A. Margirier et al.

Title Page

Abstract

Introduction

Conclusions

References

Tables

Figures



Back

Close

Full Screen / Esc

Printer-friendly Version

Interactive Discussion



Paleozoic basement. Then during the Eocene to Neogene, volcano-sedimentary deposits of the Moquegua group capped the Western Cordillera. This group is partly covered by the Huaylillas ignimbrite, produced during the Neogene volcanism. The Moquegua group and Huaylillas ignimbrite reach a maximum of 1500 m thick (Thouret et al., 2007; Gunnell et al., 2010). Some volcano-sedimentary rocks were deposited on the coastal plains during the late Neogene.

The Western Cordillera and Pacific Piedmont are incised, perpendicularly to the NW–SE Andean range, by 1 to 3 km-deep canyons (Tosdal et al., 1984; Gunnell et al., 2010; Hartley and Evenstar, 2010). This area is affected by Quaternary tectonic deformation mainly expressed in the Western Cordillera by an active fault system striking parallel to the range (Sébrier et al., 1985; Hall et al., 2008, 2012) (Fig. 2). The piedmont region is exposed to extremely low denudation rates ranging from 0.1–1 mm ka⁻¹ in the coastal desert and Pacific piedmont to 1–46 mm ka⁻¹ in the Western Cordillera (values obtained for Quaternary time-scale by TCN dating; Hall et al., 2008; Kober et al., 2007) due to the arid climate lasting at least for the Neogene (Mortimer, 1980; Alpers and Brimhall, 1988; Dunai et al., 2005). Along the Andes, the active subduction and crustal seismic activity largely control the geomorphologic evolution of the forearc (Keefer, 1994; Keefer and Moseley, 2004; Audin et al., 2006; Tavera et al., 2007; Perfettini et al., 2010). Moreover, Placzek et al. (2006, 2013) evidenced climate fluctuations on the Altiplano for the last 130 ka. Steffen et al. (2009, 2010) as well as Carretier et al. (2013) highlighted the contribution of these wet climatic events to mass transport in major canyons from the Altiplano to the Pacific coast.

2.2 Fault geometry and kinematics

In southern Peru, the Incapuquio fault zone structures the Andean range (Huaman, 1985; Sébrier et al., 1985). Based on microtectonic studies Sébrier et al. (1985, 1988) and Schildgen et al. (2009) identified different kinematic episodes. Sébrier et al. (1985, 1988) defined major Tertiary and Early Quaternary compressional phases and a minor Late Quaternary episode of normal faulting. However Schildgen et al. (2009) proposed

numerous meter-size boulders (Fig. 4a) entrapped in a thin volcanic matrix, reworked from the Huaylillas volcanic formation.

Two levels of alluvial terraces (T1, T2) and a megafan (Acoy megafan) have been identified downstream of Chuquibamba village in the Majes canyon (Fig. 3a). Their development has been linked to wetter episodes, identified in sediments of some Altiplano paleolakes (Placzek et al., 2006, 2013), driving the fluctuations of Colca/Majes hydrologic regime (Steffen et al., 2010).

3 Sampling strategy and methods

The Chuquibamba debris-flow deposit overlays the Acoy megafan in Majes valley (Figs. 3a and 4b). The megafan is about 100 m thick and 8 km long (Fig. 3a). OSL dating situates the Acoy megafan formation between 107.0 ± 5.0 ka (base) and 101.6 ± 4.9 ka (top) (Steffen et al., 2010). Its stratigraphy indicates both a response to multiple phases of sediment production and surface erosion in the Rio Grande and Majes catchments. Steffen et al. (2010) described an alternation of sheet flood units and debris-flow deposits, and a typical clast- to matrix-supported fabric. The last debris-flow deposit is perfectly preserved all along the Chuquibamba valley (Fig. 3a). Six meter-scale boulders of rhyolite entrapped in the Acoy megafan and debris-flow surfaces (Fig. 4a and c) have been sampled. The preserved surface of the boulders (evidenced by desert varnish) minimizes post-abandonment erosion; they are well-anchored and sufficiently elevated on the debris-flow surface to avoid the post-deposition movements and minimize the potential covering by surficial materials. To constrain the regional erosion rate and consequently improve the exposure age determination, we also sampled the Pampa Jahuay (quartzite pebble) in the pediplains 60 km southeast of Chuquibamba (Fig. 1 and Table 1).

Sample preparation was conducted at the Institut des Sciences de la Terre (ISTerre, Grenoble). As the rhyolitic samples contained enough quartz, we extracted in situ produced beryllium-10 (^{10}Be) using the chemical procedures developed by Brown

Title Page

Abstract

Introduction

Conclusions

References

Tables

Figures



Back

Close

Full Screen / Esc

Printer-friendly Version

Interactive Discussion



et al. (1991) and Merchel and Herpers (1999). The AMS ^{10}Be measurements were performed at the ASTER AMS French national facility (CEREGE, Aix en Provence). Analytical uncertainties include uncertainties associated with AMS counting statistics, AMS external error (1 %), standard reproducibility and chemical blank measurements ($^{10}\text{Be}/^9\text{Be}$ blank = $1.60 \pm 0.72 \times 10^{-15}$). External uncertainties include 6 % uncertainty in the production rate and 8 % uncertainty in the ^{10}Be decay constant. Exposure ages were calculated using the online Cronus Calculator (Balco et al., 2008). Results are computed using the time dependent scaling scheme of Lal (1991) modified by Stone (2000).

4 Results

The upper destabilization zone is composed of imbricated rotational landslides (Fig. 3b). The rotational landslides boundary corresponds to a succession of 3 head scarps (located at ~ 3700 m a.s.l.), which form an elongated amphitheater shaped scar trending in the NW–SE direction. This direction does not fit with the overall South/West orientation of the topographic slope, but rather corresponds to the structural trend of active faults (Fig. 3a). Moreover several fault planes control the shape of the polylobed rotational landslides (Fig. 3b). The base of the cirque (2900 m a.s.l.) is formed by smooth and sub horizontal surfaces (Fig. 3b). This would correspond to former lateral landslide deposits re-incised by the river after the initiation of the Chuquibamba landslide. The debris-flow deposit consists of large boulders embedded in a thin matrix and displays a smooth and 100 m-scale undulated surface (Fig. 4a). In its upper part, this debris-flow rests directly on the basement (Fig. 4a); but 30 km downstream of the head scarp, in the vicinity of the Majes River (900 m a.s.l.), the debris-flow rests on the Acoy megafan (Figs. 3a and 4). The ^{10}Be concentrations are relatively consistent and range from $6.67 \pm 0.28 \times 10^5$ to $1.38 \pm 0.08 \times 10^6$ atoms per gram of quartz (at g^{-1} qtz) (Table 1). It is important to note that the associated analytical uncertainties are remarkably low (3–6 %), probably due to the purity of the quartz mineral, allowing low interferences

Title Page

Abstract

Introduction

Conclusions

References

Tables

Figures

◀

▶

◀

▶

Back

Close

Full Screen / Esc

Printer-friendly Version

Interactive Discussion



Tectonic and climatic

A. Margirier et al.

Title Page

Abstract

Introduction

Conclusions

References

Tables

Figures

◀

▶

◀

▶

Back

Close

Full Screen / Esc

Printer-friendly Version

Interactive Discussion



during AMS measurement and subsequently excellent analytical statistics (Table 1). The high ^{10}Be content of the sample ($1.33 \pm 0.02 \times 10^7 \text{ atg}^{-1} \text{ qtz}$, 11A28) collected in the Pampa Jahuay suggests an extremely low erosion rate lasting at least for the last 2 million years in the southern Peruvian forearc ($1.9 \pm 0.3 \text{ My}$). The computed erosion rate ($0.21 \pm 0.05 \text{ mm ka}^{-1}$) agrees with rates published by Hall et al. (2012) and, for Chile, by Kober et al. (2007). This supports the hypothesis of a non-significant erosion of the sampled boulders of the debris-flow deposit. TCN exposure ages deduced from debris-flow boulders range from 96.1 ± 8.9 to 108.5 ± 10.2 ^{10}Be -ka (Table 1, Fig. 5). Considering the uncertainties, exposure ages are consistent and suggest a single remobilization event with a weighted average age of $101.9 \pm 5.5 \text{ ka}$. The age of the large boulder sampled on the Acoy megafan (Fig. 4) is 105.3 ± 10.2 ^{10}Be -ka (Table 1).

5 Discussion

5.1 Tectonic and climatic forcing on Chuquibamba landslide evolution

The weighted average age of debris-flow boulders indicates a last major debris-flow at $101.9 \pm 5.5 \text{ ka}$. The abandonment age of the megafan surface (105.3 ± 10.2 ^{10}Be -ka; Figs. 4 and 5) agrees with the OSL ages published by Steffen et al. (2010) (i.e. $107.0 \pm 5.0 \text{ ka}$ at the base of the megafan and $101.6 \pm 4.9 \text{ ka}$ near the top). The Ouki wet event has been evidenced from sediments collected in the eponym paleolake located in the higher Bolivian Altiplano (Placzek et al., 2006, 2013). The chronological framework deduced from U-Th dating on carbonates indicates the Ouki deep lake cycle between 120 to 98 ka (Placzek et al., 2006, 2013). Steffen et al. (2010) already suggested a correlation between wet time intervals on the Altiplano and sediment aggradation in the Majes Valley; they linked the Acoy megafan formation to the Ouki wet climatic event. After Steffen et al. (2010), the Acoy megafan recorded two phases of catchment development characterized by landsliding. Similarly to Lluta catchment in Chile, landsliding might have been initiated by enhanced precipitation and a reduced

Tectonic and climatic

A. Margirier et al.

basal shear stress due to increasing hydrostatic pressure in the groundwater (Hoke et al., 2004; Strasser and Schlunegger, 2005). The weighted average age of the last debris-flow deposit (101.9 ± 5.5 ka) also correlates with the Ouki event (120–98 ka). In the western Andes, other landslides have been associated with wet events such as the older Tomasiri landslide (South Peru; $17^{\circ}30'$ S), dated at 400 ka (Blard et al., 2009) or younger Argentinian landslides which have been associated with the Minchin event (40–25 ka; Trauth et al., 2003; Hermanns and Schellenberger, 2008). We suggest that the debris-flow, which remobilized rotational landslide deposits, was triggered by an increase in the pore water pressure at the base of the Huayllillas Ignimbrites during the Ouki wet climatic event.

The link between the tectonic framework, localization and flow direction of a mega-landslide, has already been suggested in the Andean forearc domain (Pinto et al., 2008; Antinao and Gosse, 2009; Mather et al., 2014). As the Chuquibamba landslide is elongated in an NW–SE trend guided by the Incapuquio fault system we suggest that the localization and geometry of landslides are mainly controlled by preferential fracturing orientations (Fig. 3b).

No relation between a $M_w = 8.0$ subduction earthquake and giant-landslide has been previously evidenced in southern Peru (Lacroix et al., 2013) but Keefer et al. (2003) point out that the succession in time of subduction earthquakes and El Nino events produces debris-flows in the coastal region (southern Peru). Here a likely link seems to be established between the recurrence of seismicity and landslide triggering. Even if the Ouki wet phase seems to predispose the triggering, we can not exclude a seismic triggering (subduction or crustal earthquake) for the Chuquibamba debris-flows. More generally, robust arguments indicating such a correlation for giant-landslides are scarce along the South American margin, other triggering factors (increase of pore pressure, climate change, glacial debuttressing) are usually invoked in addition to a seismic triggering (Keefer, 2002; Pinto et al., 2008).

Title Page

Abstract

Introduction

Conclusions

References

Tables

Figures

◀

▶

◀

▶

Back

Close

Full Screen / Esc

Printer-friendly Version

Interactive Discussion



5.2 Landscape evolution and tectono-climatic scenario

We propose a landscape evolution scenario based on geomorphic marker analysis and new TCN ages (Fig. 6). The initial drainage network flowed toward the coast (i.e. in a southerly direction) and incised the Huaylillas paleosurface (Fig. 6a). These parallel incisions are still preserved (Fig. 3b) and sometimes even abandoned. Afterwards, the development of a graben structured by the Incapuquio fault system captured the drainage network along a 110° N trending direction (Fig. 3c) creating a new tributary of the Majes River. Rotational landslides were initiated by slope instability or pore pressure increase at the base of the Huaylillas ignimbrite during wet climatic events as proposed by Hoke et al. (2004) and Strasser and Schlunegger (2005) for northern Chile (Fig. 6b). Sliding surfaces of rotational landslides are localized on fault planes and progressively enlarge the valley as evidenced by the successive rotational landslides scarps (Fig. 3).

The rotational landslides deposits accumulate upstream in the valley (Fig. 6b) and were remobilized by debris-flows during the Ouki event (120–98 ka; Fig. 6c). The accumulation of successive debris-flow and mudflow deposits at the outlet of the Rio Grande during the Ouki event formed the Acoy megafan (Steffen et al., 2010). Finally, 101.9 ka ago, the last major debris-flow sealed the erosion/transport system (Fig. 6c). This last debris-flow permits new destabilizations that enlarge the system (Fig. 6d). At the present time, the arid climate on the western flank of the Cordillera preserves geomorphologic features from erosion, the water yield comes only from rivers. The debris-flow deposit surface is perfectly preserved; the Rio Grande just incises the debris-flow deposit (~ 100 m) due to the lack of a significant input of water issuing from the Western Cordillera.

ESURFD

2, 1129–1153, 2014

Tectonic and climatic

A. Margirier et al.

Title Page

Abstract

Introduction

Conclusions

References

Tables

Figures

◀

▶

◀

▶

Back

Close

Full Screen / Esc

Printer-friendly Version

Interactive Discussion



6 Conclusions

In an arid context, Terrestrial Cosmogenic Nuclides are the perfect tool to date the exposure of surface older than ~ 100 ka. In the Peruvian arid piedmont, the TCN dating of landslides is theoretically applicable over several hundreds of thousands of years, particularly in this case of gigantic boulder sampling. Additionally our data exemplify that quartz crystals extracted from rhyolites are particularly adapted to TCN dating and open new perspectives for quantitative geomorphologic applications in volcanic areas.

This study raises the question of the control of local tectonic activity and Altiplano climatic fluctuations on landslide processes in the arid western Andean front. Indeed, for the Chuquibamba landslide region, the last debris-flow (101.9 ka) seems to have been favored by the occurrence of a wet climatic event (Ouki event), even if a seismic triggering cannot be excluded. Wet climatic events appear to control the growth of the drainage network, participating in regressive erosive events and the creation of new tributaries on the western Andean front. Our results also show that during wet events in a tectonically fractured region, hillslope processes, rather than fluvial erosion, dictate the evolution of the landscape at the channel head in the arid and high relief area. Our results suggest sediment accumulation in the valley during wet periods and incision during dry periods.

More broadly, in southern Peru and northern Chile most of the large landslides are located in tectonically fractured regions. In these arid regions, climatic fluctuations have a greater impact on landslide triggering and on sediment transport. Carretier et al. (2013) proposed that the contribution of rare and strong erosive events to the long-term erosion of the Andean range is more than 90% in an arid climatic context. As massive landslides disrupting the arid western Andean front represent an important contribution to long-term Andean range erosion, we suggest a strong regional tectonic and climatic control of the long-term erosion of the arid western Andean front.

An important perspective of this study would be the systematic dating of the massive landslides disrupting the western Andean front to quantify the long-term erosion rates.

Title Page

Abstract

Introduction

Conclusions

References

Tables

Figures



Back

Close

Full Screen / Esc

Printer-friendly Version

Interactive Discussion



Acknowledgements. This project was supported by the Institut de Recherche pour le Développement (IRD). We acknowledge additional support from Instituto Geologico Minero-metalurgico y Metallurgico del Peru (INGEMMET, Peru). We thank all the staff from the ASTER AMS facility at CEREGE. This work has been carried out in the frame of the Master Thesis of A. Margirier in ISTERre.

References

- Alpers, C. N. and Brimhall, G. H.: Middle Miocene climatic change in the Atacama Desert, northern Chile: Evidence from supergene mineralization at La Escondida, *Geol. Soc. Am. Bull.*, 100, 1640–1656, 1988.
- Antinao, J. L. and Gosse, J.: Large rockslides in the Southern Central Andes of Chile (32–34.5° S): tectonic control and significance for Quaternary landscape evolution, *Geomorphology*, 104, 117–133, 2009.
- Atherton, M. P., Warden, V., and Sanderson, L. M.: The Mesozoic marginal basin of Central Peru: a geochemical study of within-plate-edge volcanism, in: *Magmatism at a Plate Edge: the Peruvian Andes*, edited by: Pitcher, M. P., Cobbing, E. J., and Beckinsale, R. D., Blackie Halsted Press, London, 47–58, 1985.
- Audin, L. and Bechir, A.: Active Tectonics as Determinant Factor in Landslides Along the western Cordillera?, *Congreso Peruano de Geologia*, Lima, Peru, 17–20 October, 237–239, 2006.
- Audin, L., David, C., Hall, S., Farber, D., and Hérial, G.: Geomorphic evidences of recent tectonic activity in the forearc, southern Peru, Special Volume on Neotectonics in South America, *Revista de la Asociación Geológica Argentina*, 61, 545–554, 2006.
- Balco, G., Stone, J. O., Lifton, N. A., and Dunai, T. J.: A complete and easily accessible means of calculating surface exposure ages or erosion rates from ^{10}Be and ^{26}Al measurements, *Quat. Geochronol.*, 3, 174–195, 2008.
- Blard, P. H., Lavé, J., Farley, K. A., Fornari, M., Jiménez, N., and Ramirez, V.: Late local glacial maximum in the Central Altiplano triggered by cold and locally-wet conditions during the paleolake Tauca episode (17–15 ka, Heinrich 1), *Quaternary Sci. Rev.*, 28, 3414–3427, 2009.

ESURFD

2, 1129–1153, 2014

Tectonic and climatic

A. Margirier et al.

Title Page

Abstract

Introduction

Conclusions

References

Tables

Figures

◀

▶

◀

▶

Back

Close

Full Screen / Esc

Printer-friendly Version

Interactive Discussion



Tectonic and climatic

A. Margirier et al.

Title Page

Abstract

Introduction

Conclusions

References

Tables

Figures

I◀

▶I

◀

▶

Back

Close

Full Screen / Esc

Printer-friendly Version

Interactive Discussion



Brown, E. T., Edmond, J. M., Raisbeck, G. M., Yiou, F., Kurz, M. D., and Brook, E. J.: Examination of surface exposure ages of Antarctic moraines using in situ produced ^{10}Be and ^{26}Al , *Geochim. Cosmochim. Ac.*, 55, 2269–2283, 1991.

Carretier, S., Regard, V., Vassallo, R., Aguilar, G., Martinod, J., Riquelme, R., Pepin, E., Charrier, R., Hérail, G., Farias, M., Guyot, J. L., Vargas, G., and Lagane, C.: Slope and climate variability control of erosion in the Andes of central Chile, *Geology*, 41, 195–198, 2013.

Chmeleff, J., von Blanckenburg, F., Kossert, K., and Jacob, D.: Determination of the ^{10}Be half-life by multicollector ICP-MS and liquid scintillation counting, *Nucl. Instrum. Methods*, 268, 192–199, 2010.

Devlin, S., Isacks, B. L., Pritchard, M. E., Barnhart, W. D., and Lohman, R. B.: Depths and focal mechanisms of crustal earthquakes in the central Andes determined from teleseismic waveform analysis and InSAR, *Tectonics*, 31, TC2002, doi:10.1029/2011TC002914, 2012.

Crosta, G. B., Paolo, F., Elena, V., and Hermanns, R. L.: The Cerro Caquilluco–Cerrillos Negros Giant Rock Avalanches (Tacna, Peru), *Engineering Geology for Society and Territory*, 2, 921–924, doi:10.1007/978-3-319-09057-3_159, 2015.

Dunai, T. J., González López, G. A., and Juez-Larré, J.: Oligocene-Miocene age of aridity in the Atacama Desert revealed by exposure dating of erosion-sensitive landforms, *Geology*, 33, 321–324, 2005.

Grange, F., Hatzfeld, D., Cunningham, P., Molnar, P., Roecker, S. W., Suarez, G., Rodrigues, A., and Ocola, L.: Tectonic implications of the microearthquake seismicity and fault plane solutions in southern Peru, *J. Geophys. Res.*, 89, 6139–6152, 1984.

Gunnell, Y., Thouret, J. C., Brichau, S., Carter, A., and Gallagher, K.: Low-temperature thermochronology in the Peruvian Central Andes: implications for long-term continental denudation, timing of plateau uplift, canyon incision and lithosphere dynamics, *J. Geol. Soc. London*, 167, 803–815, 2010.

Guzzetti, F., Mondini, A. C., Cardinali, M., Fiorucci, F., Santangelo, M., and Chang, K.-T.: Landslide inventory maps: new tools for an old problem, *Earth-Sci. Rev.*, 112, 1–25, 2012.

Hall, S. R., Farber, D. L., Audin, L., Finkel, R. C., and Mériaux, A. S.: Geochronology of pediment surfaces in southern Peru: implications for Quaternary deformation of the Andean forearc, *Tectonophysics*, 459, 186–205, 2008.

Hall, S. R., Farber, D. L., Audin, L., and Finkel, R. C.: Recently active contractile deformation in the forearc of southern Peru, *Earth Planet. Sc. Lett.*, 337–338, 85–92, 2012.

Tectonic and climatic

A. Margirier et al.

Title Page

Abstract

Introduction

Conclusions

References

Tables

Figures

I◀

▶I

◀

▶

Back

Close

Full Screen / Esc

Printer-friendly Version

Interactive Discussion



Hartley, A. J. and Evenstar, L.: Cenozoic stratigraphic development in the north Chilean forearc: implications for basin development and uplift history of the Central Andean margin, *Tectonophysics*, 495, 67–77, 2010.

Hermanns, R. L. and Schellenberger, A.: Quaternary tephrochronology helps define conditioning factors and triggering mechanisms of rock avalanches in NW Argentina, *Quatern. Int.*, 178, 261–275, 2008.

Hoke, G. D., Isacks, B. L., Jordan, T. E., and Yu, J. S.: Groundwater-sapping origin for the giant quebradas of northern Chile, *Geology*, 32, 605–608, 2004.

Hovius, N., Meunier, P., Ching-Weei, L., Hongey, C., Yue-Gau, C., Dadson, S., Ming-Jame, H., and Lines, M.: Prolonged seismically induced erosion and the mass balance of a large earthquake, *Earth Planet. Sc. Lett.*, 304, 347–355, 2011.

Huaman, R.: Evolution tectonique Cenozoïque et néotectonique du piémont Pacifique dans la région d'Arequipa (Andes du Sud Pérou), Ph.D. thesis, Université Paris Sud, Centre d'Orsay, 220 pp., 1985.

INGEMMET: Mapa Geológico del cuadrángulo de Caravelí, Ocoña, La Yesera, y Chuquibamba, scale 1 : 100 000, Lima, 2001.

Keefer, D. K.: Landslides caused by earthquakes, *Geol. Soc. Am. Bull.*, 95, 406–421, 1984.

Keefer, D. K.: The importance of earthquake-induced landslides to long-term slope erosion and slope-failure hazards in seismically active regions, *Geomorphology*, 10, 265–284, 1994.

Keefer, D. K.: Investigating landslides caused by earthquakes – a historical review, *Surv. Geophys.*, 23, 473–510, 2002.

Keefer, D. K. and Moseley, M. E.: Southern Peru desert shattered by the great 2001 earthquake: implications for paleoseismic and paleo-El Niño-Southern Oscillation records, *P. Natl. Acad. Sci. USA*, 101, 10878–10883, 2004.

Keefer, D. K., Moseley, M. E., and deFrance, S. D.: A 38 000 year record of floods and debris flows in the Ilo region of southern Peru and its relation to El Niño events and great earthquakes, *Palaeogeogr. Palaeoclimatol.*, 194, 41–77, 2003.

Kelly, M. A., Lowell, T. V., Applegate, P. J., Phillips, F. M., Schaefer, J. M., Smith, C. A., Kim, H., Leonard, K. C., and Hudson, A. M.: A locally calibrated, late glacial ^{10}Be production rate from a low-latitude, high-altitude site in the Peruvian Andes, *Quat. Geochronol.*, 1–16, in press, 2014.

Tectonic and climatic

A. Margirier et al.

Title Page

Abstract

Introduction

Conclusions

References

Tables

Figures



Back

Close

Full Screen / Esc

Printer-friendly Version

Interactive Discussion



- Kober, F., Ivy-Ochs, S., Schlunegger, F., Baur, H., Kubik, P. W., and Wieler, R.: Denudation rates and a topography-driven rainfall threshold in northern Chile: multiple cosmogenic nuclide data and sediment yield budgets, *Geomorphology*, 83, 97–120, 2007.
- Korschinek, G., Bergmaier, A., Faestermann, T., Gerstmann, U. C., Knie, K., Rugel, G., Wallner, A., Dillmann, I., Dollinger, G., Gostomski von C. L., Kossert, K., Maiti, M., Poutivtsev, M., and Remmert, A.: A new value for the half-life of ^{10}Be by heavy-ion elastic recoil detection and liquid scintillation counting, *Nuclear Instrum. Methods*, 268, 187–191, 2010.
- Korup, O., Clague, J. J., Hermanns, R. L., Hewitt, K., Strom, A. L., and Weidinger, J. T.: Giant landslides, topography, and erosion, *Earth Planet. Sc. Lett.*, 261, 578–589, 2007.
- Lacroix, P., Zavala, B., Berthier, E., and Audin, L.: Supervised method of landslide inventory using panchromatic SPOT5 images and application to the earthquake-triggered landslides of Pisco (Peru, 2007, M_w 8.0), *Remote Sensing*, 5, 2590–2616, 2013.
- Lal, D.: Cosmic ray labeling of erosion surfaces: in situ nuclide production rates and erosion models, *Earth Planet. Sc. Lett.*, 104, 24–439, 1991.
- Mather, A. E., Hartley, A. J., and Griffiths, J. S.: The giant landslides of northern Chile: tectonic and climate interactions on a classic convergent plate margin, *Earth Planet. Sc. Lett.*, 388, 249–256, 2014.
- Meunier, P., Hovius, N., and Haines, J. A.: Topographic site effects on the location of earthquake induced landslides, *Earth Planet. Sc. Lett.*, 275, 221–232, 2008.
- Merchel, S. and Herpers, U.: An update on radiochemical separation techniques for the determination of long-lived radionuclides via accelerator mass spectrometry, *Radiochim. Acta*, 84, 215–219, 1999.
- Mortimer, C.: Drainage evolution of the Atacama Desert of northernmost Chile, *Rev. Geol. Chile*, 11, 3–28, 1980.
- Perfettini, H., Vouac, J.-P., Tavera, H., Kositsky, A., Nocquet, J.-M., Bondoux, F., Chlieh, M., Sladen, A., Audin, L., and Farber, D. L.: Seismic and aseismic slip on the central Peru megathrust, *Nature*, 465, 78–81, 2010.
- Pinto, L., Hérail, G., Sepúlveda, S. A., and Krop, P.: A neogene giant landslide in Tarapacá, northern Chile: a signal of instability of the westernmost Altiplano and palaeoseismicity effects, *Geomorphology*, 102, 532–541, 2008.
- Placzek, C., Quade, J., and Patchett, P. J.: Geochronology and stratigraphy of late Pleistocene lake cycles on the southern Bolivian Altiplano: implications for causes of tropical climate change, *Geol. Soc. Am. Bull.*, 118, 515–532, 2006.

Tectonic and climatic

A. Margirier et al.

Title Page

Abstract

Introduction

Conclusions

References

Tables

Figures

◀

▶

◀

▶

Back

Close

Full Screen / Esc

Printer-friendly Version

Interactive Discussion



- Placzek, C. J., Quade, J., and Patchett, P. J.: A 130 ka reconstruction of rainfall on the Bolivian Altiplano: implications for the causes of tropical climate change, *Earth Planet. Sc. Lett.*, 363, 97–108, 2013.
- 5 Roperch, P., Sempere, T., Macedo, O., Arriagada, C., Fornari, M., Tapia, C., Garcia, M., and Laj, C.: Counterclockwise rotation of late Eocene–Oligocene fore-arc deposits in southern Peru and its significance for oroclinal bending in the central Andes, *Tectonics*, 25, TC3010, doi:10.1029/2005TC001882, 2006.
- 10 Schildgen, T. F., Hodges, K. V., Whipple, K. X., Pringle, M. S., van Soest, M., and Cornell, K.: Late Cenozoic structural and tectonic development of the western margin of the central Andean Plateau in southwest Peru, *Tectonics*, 28, TC4007, doi:10.1029/2008TC002403, 2009.
- Sébrier, M., Mercier, J. L., Mégard, F., Laubacher, G., and Carey-Gailhardis, E.: Quaternary normal and reverse faulting and the state of stress in the central Andes of south Peru, *Tectonics*, 4, 739–780, 1985.
- 15 Sébrier M., Lavenu, A., Fornari, M., and Soulas, J. P.: Tectonics and uplift in Central Andes (Peru, Bolivia and Northern Chile) from Eocene to present, *Géodynamique*, 3, 85–106, 1988.
- Steffen, D., Schlunegger, F., and Preusser, F.: Drainage basin response to climate change in the Pisco valley, Peru, *Geology*, 37, 491–494, 2009.
- Steffen, D., Schlunegger, F., and Preusser, F.: Late Pleistocene fans and terraces in the Majes valley (southern Peru) and their relation to climatic variations, *Int. J. Earth Sci.*, 99, 1975–2010, 2010.
- 20 Stone, J. O.: Air pressure and cosmogenic isotope production, *J. Geophys. Res.*, 105, 23753–23759, 2000.
- Strasser, M. and Schlunegger, F.: Erosional processes, topographic length-scales and geomorphic evolution in arid climatic environments: the “Lluta collapse,” northern Chile, *Int. J. Earth Sci.*, 94, 433–446, 2005.
- 25 Tavera, H., Audin, L., and Bernal, I.: Source parameters of Sama (Tacna) earthquake (5.4 M_w) of 20 November 2006, *Bol. Soc. geol. Perú*, 102, 109–115, 2007.
- Thouret, J. C., Wörner, G., Gunnell, Y., Singer, B., Zhang, X., and Souriot, T.: Geochronologic and stratigraphic constraints on canyon incision and Miocene uplift of the Central Andes in Peru, *Earth Planet. Sc. Lett.*, 263, 151–166, 2007.
- 30 Tosdal, R. M., Clark, A. H., and Farrar, E.: Cenozoic polyphase landscape and tectonic evolution of the Cordillera Occidental, southernmost Peru, *Geol. Soc. Am. Bull.*, 95, 1318–1332, 1984.

Trauth, M. H., Bookhagen, B., Marwan, N., and Strecker, M. R.: Multiple landslide clusters record Quaternary climate changes in the northwestern Argentine Andes, *Palaeogeogr. Palaeoclimatol.*, 194, 109–121, 2003.

5 Victor, P., Oncken, O., and Glodny, J.: Uplift of the western Altiplano plateau: evidence from the Precordillera between 20 and 21° S (northern Chile), *Tectonics*, 23, TC4004, doi:10.1029/2003TC001519, 2004.

Wörner, G., Uhlig, D., Kohler, I., and Seyfried, H.: Evolution of the West Andean Escarpment at 18° S (N. Chile) during the last 25 Ma: uplift, erosion and collapse through time, *Tectonophysics*, 345, 183–198, 2002.

ESURFD

2, 1129–1153, 2014

Tectonic and climatic

A. Margirier et al.

Title Page

Abstract

Introduction

Conclusions

References

Tables

Figures



Back

Close

Full Screen / Esc

Printer-friendly Version

Interactive Discussion



Sample	Latitude (° N)	Longitude (° W)	Elevation (m a.s.l.)	Production rate (atoms g ⁻¹ yr ⁻¹)	Geomorphic scaling factor (a)	Sample thickness factor (b)	Quartz (g)	⁹ Be (mg)	¹⁰ Be/ ⁹ Be (c)	Uncertainty ¹⁰ Be/ ⁹ Be (%)	¹⁰ Be concentration (×10 ³ atoms g ⁻¹ Qtz)	
				Spallation	Muons							
Blank												
BKGRE67	–	–	–	–	–	–	–	0.486	1.604 × 10 ⁻¹⁵	44.74	31.374	
Debris-flow deposit												
11A39	–15.9294	–72.5306	1315	7.15	0.27	0.99	0.98	9.54	0.291	3.998 × 10 ⁻¹³	3.10	828.574
11A40	–15.5327	–72.9267	1356	7.43	0.28	0.99	0.99	6.02	0.254	3.257 × 10 ⁻¹³	3.16	938.088
11A41	–15.5343	–72.9245	1391	7.39	0.28	0.98	0.97	5.10	0.290	2.566 × 10 ⁻¹³	3.52	992.821
11A42	–15.9145	–72.5487	1543	8.40	0.29	0.99	0.98	10.98	0.292	5.468 × 10 ⁻¹³	3.44	992.144
11A43	–15.8784	–72.5927	1899	10.54	0.33	0.98	0.98	10.44	0.291	6.981 × 10 ⁻¹³	6.14	1375.656
Acroy megafan												
11A28	–16.0091	–72.4892	817	5.13	0.24	1.00	0.99	9.77	0.294	3.196 × 10 ⁻¹³	4.18	666.607
Pampa Jahuary												
11A62	–16.3408	–72.0840	1592	8.76	0.30	1.00	0.97	19.96	0.295	1.320 × 10 ⁻¹¹	1.71	13318.936

Sample	¹⁰ Be concentration uncertainty (×10 ³ atoms g ⁻¹ Qtz)	Erosion rate (m Ma ⁻¹)	Erosion rate external uncertainty (m Ma ⁻¹)	Age ¹⁰ Be (ka) e = 0 (d)	Age ¹⁰ Be internal uncertainty (ka) (e)	Age ¹⁰ Be external uncertainty (ka) (f)	Age ¹⁰ Be (ka) e = 0.21 m Ma ⁻¹ (d)	Age ¹⁰ Be internal uncertainty (ka) (e)	Age ¹⁰ Be external uncertainty (ka) (f)
Blank									
BKGRE67	14.036	–	–	–	–	–	–	–	–
Debris-flow deposit									
11A39	25.748	–	–	95.99	3.67	8.83	96.11	3.68	8.86
11A40	29.597	–	–	102.72	4.07	9.49	102.86	4.09	9.52
11A41	34.974	–	–	108.29	4.85	10.17	108.46	4.87	10.2
11A42	34.175	–	–	97.51	4.17	9.10	97.88	4.19	9.15
11A43	84.507	–	–	106.7	8.30	11.42	106.87	8.34	11.46
Acroy megafan									
11A28	27.905	–	–	105.1	5.55	10.15	105.26	5.57	10.19
Pampa Jahuary									
11A62	227.531	0.21	0.05	1894.08	94.88	271.34	–	–	–

Title Page

Abstract

Introduction

Conclusions

References

Tables

Figures



Back

Close

Full Screen / Esc

Printer-friendly Version

Interactive Discussion



Tectonic and climatic

A. Margirier et al.

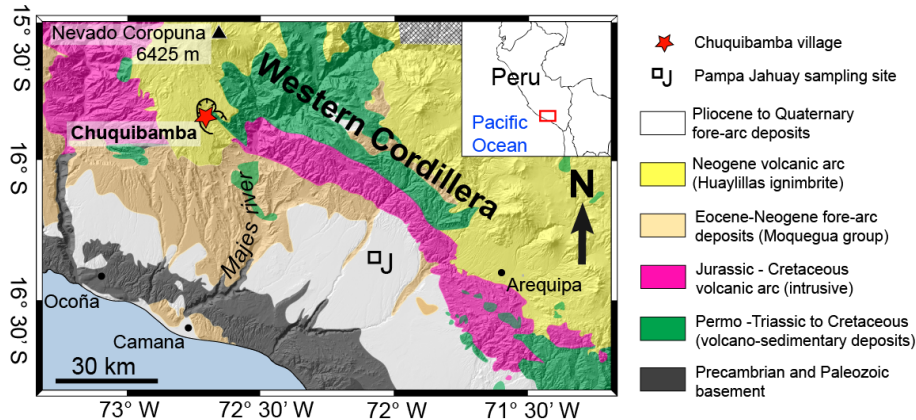


Figure 1. Simplified geological map of South Peru (INGEMMET, 2001; modified from Rop-erch et al., 2006), showing the Chuquibamba village (red star), the destabilization zone and the Pampa Jahuay sampling site (J). Coordinates are given in WGS 84 longitude and latitude (degrees). Inset shows the study area location within Peru and a part of South America.

Title Page	
Abstract	Introduction
Conclusions	References
Tables	Figures
◀	▶
◀	▶
Back	Close
Full Screen / Esc	
Printer-friendly Version	
Interactive Discussion	



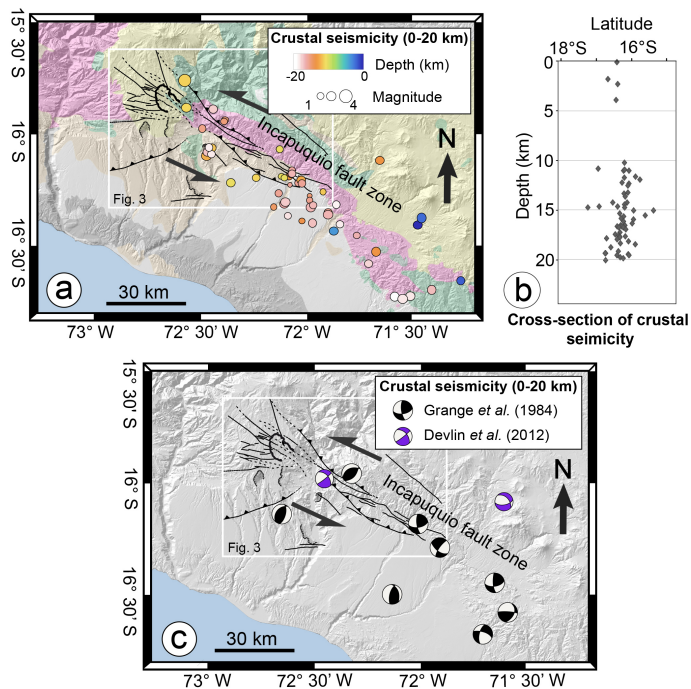


Figure 2. Regional crustal seismicity and focal mechanisms. **(a)** Crustal seismicity (depth < 20 km) and faults are represented on the geological map of South Peru (INGEMMET, 2001; modified from Roperch et al., 2006). **(b)** Cross section showing the vertical cluster of earthquakes. **(c)** Focal mechanisms from Grange et al. (1984) and Devlin et al. (2012) studies, the kinematic of the Incapuquio fault system is indicated by black arrows.



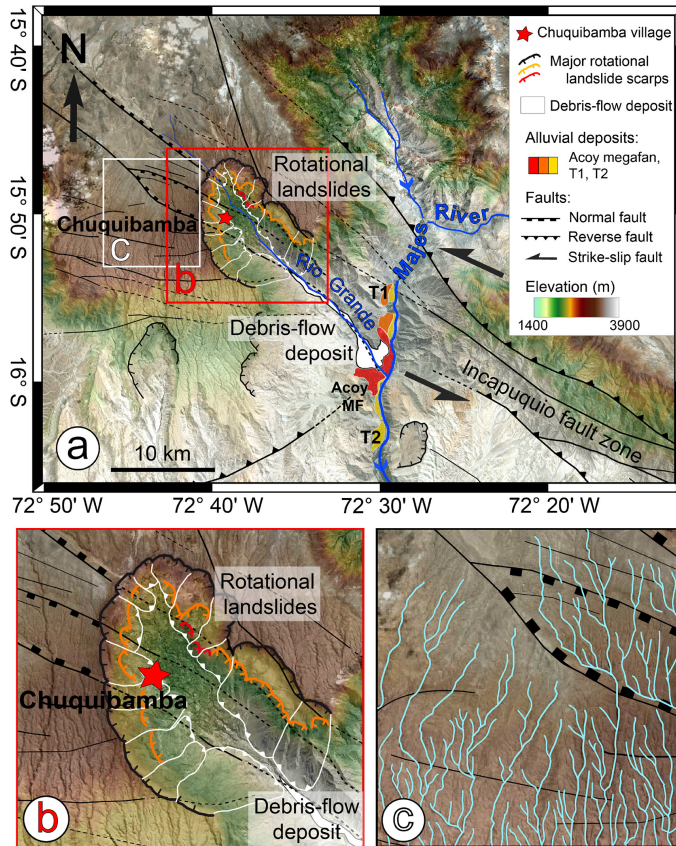


Figure 3. SRTM numerical elevation model overlay by Landsat image of the Chuquibamba destabilization zone. Coordinates are given in WGS 84 longitude and latitude (degrees). **(a)** Global view of the Chuquibamba area pointing major detachment scarps, debris-flow deposits, Acoy megafan, alluvial terraces and faults. **(b)** Zoom on the amphitheater-shaped scar of the rotational landslides showing the different head scarps. **(c)** Drainage network and faults.

Title Page

Abstract

Introduction

Conclusions

References

Tables

Figures

◀

▶

◀

▶

Back

Close

Full Screen / Esc

Printer-friendly Version

Interactive Discussion



Tectonic and climatic

A. Margirier et al.

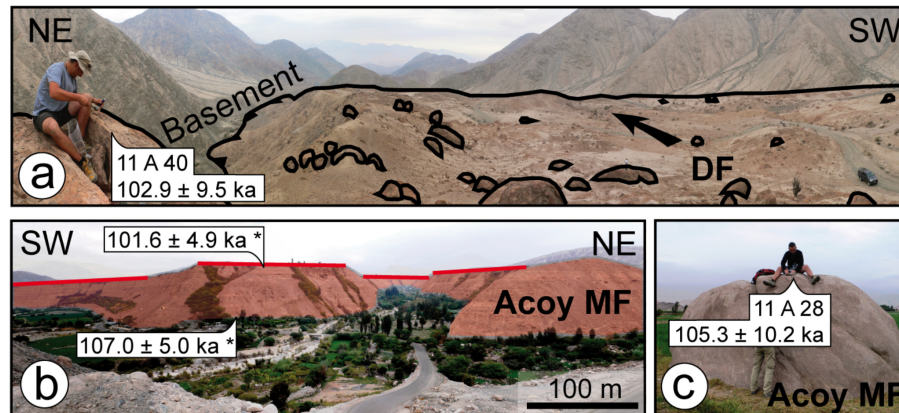


Figure 4. Field photographs showing the debris-flow deposit morphology and the Acoy megafan. **(a)** Characteristic block sampled on the debris-flow deposit. The arrow indicates flowing direction of the debris-flow. **(b)** General view of the Acoy megafan (Acoy MF), red lines highlight the top of the terrace. The OSL ages obtain by Steffen et al. (2010) for the Acoy megafan are indicated with an asterisk **(c)** Block sampled on the megafan.

Title Page

Abstract

Introduction

Conclusions

References

Tables

Figures

I◀

▶I

◀

▶

Back

Close

Full Screen / Esc

Printer-friendly Version

Interactive Discussion



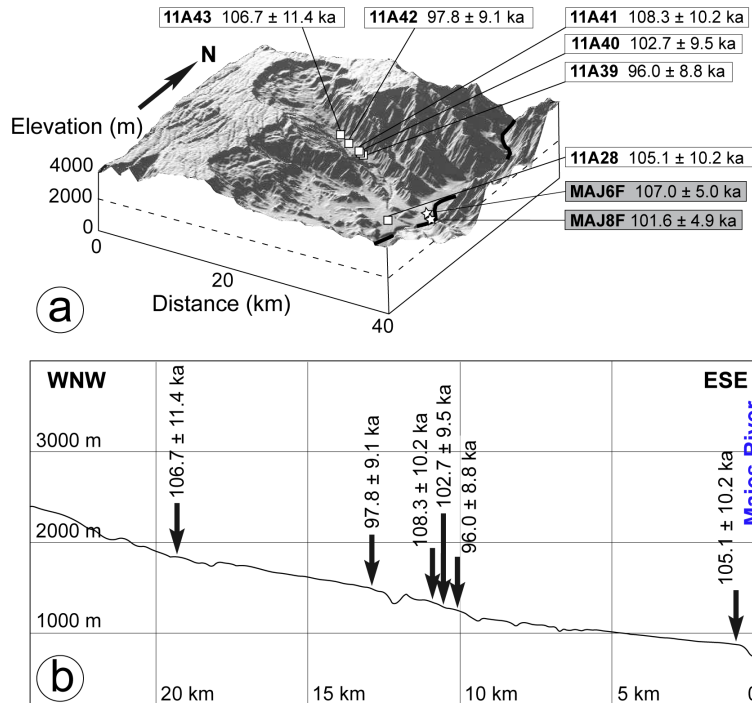


Figure 5. Samples location. **(a)** Digital elevation model (GeoMapApp, SRTM data, 90 m resolution) of the study area, showing samples location and TCN ages obtained for the debris-flow deposit and the Acyco megafan surface. OSL ages obtained by (Steffen et al., 2010) for the Acyco megafan are noted in grey. **(b)** Elevation profile locating debris-flow and the Acyco megafan ages.



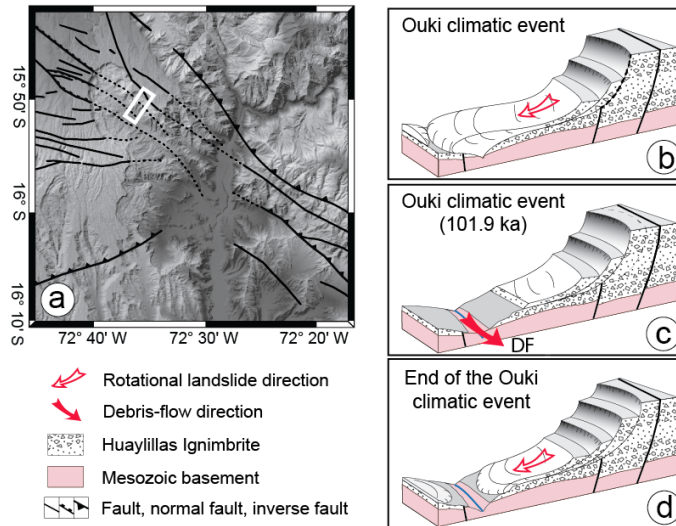


Figure 6. Map and block diagrams of the evolution of the Chuquibamba landslide. **(a)** SRTM numerical elevation model, the white rectangle localizes the block diagrams. **(b)** Block diagram showing rotational landslide initiation on the flank of the Chuquibamba Valley during the Ouki wet event. The landslide enlarges the valley and accumulates material at the bottom. **(c)** The accumulated materials are remobilized by debris-flows during the wetter phases. **(d)** This remobilization allows new rotational landslides that enlarge the amphitheater shape valley.